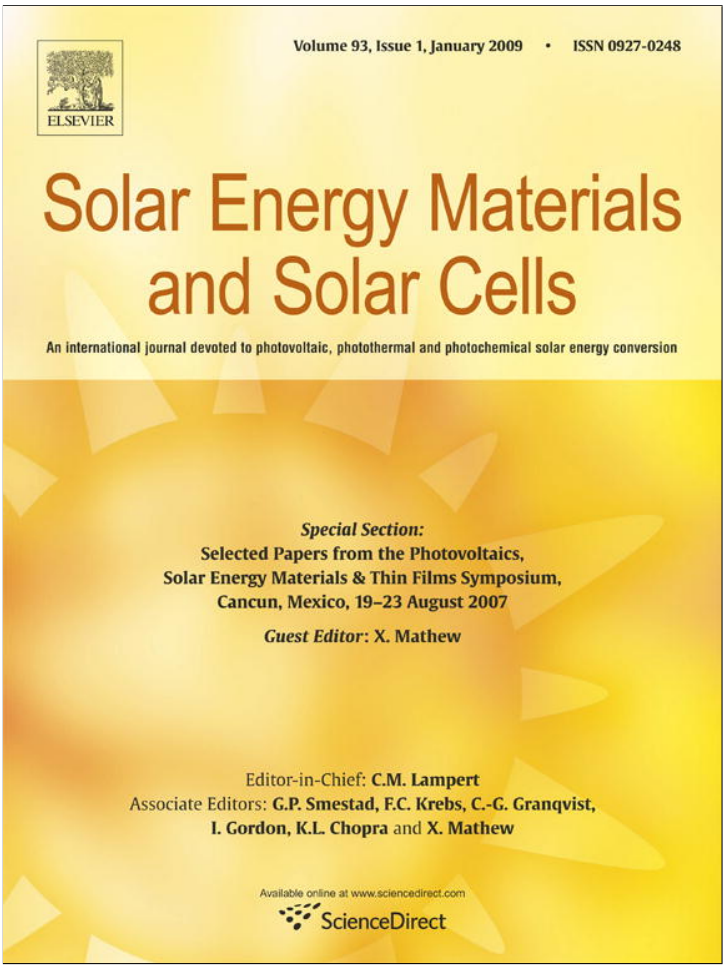

Solar Energy Materials & Solar Cells 93 (2009) 85–91

Contents lists available at ScienceDirect

Solar Energy Materials & Solar Cells

journal homepage: www.elsevier.com/locate/solmat

Spherical antireflection coatings by large-area convective assembly of monolayer silica microspheres

Y. Wang [a,b,*,1], L. Chen [a], H. Yang [a], Q. Guo [c], W. Zhou [a,*], M. Tao [a,c,2,*]

[a] Department of Electrical Engineering, NanoFAB Center, University of Texas at Arlington, Arlington, TX 76019-0072, USA
[b] Department of Chemistry and Biology, University of Electronic Science and Technology of China, Zhongshan Institute, Zhongshan 528402, China
[c] ZT Solar, Inc., 1120 South Freeway, Fort Worth, TX 76104, USA

ARTICLE INFO

Article history:
Received 4 June 2008
Accepted 5 August 2008
Available online 8 October 2008

Keywords:
Microparticle
Convective assembly
Monolayer
Antireflection coating
Solar cell

ABSTRACT

Solution-processed surface textures are highly desirable for antireflection in high-performance cost-effective solar cells. Inorganic spherical surface textures can be formed with monolayers of microscale silica spheres partially immersed into spin-on-glass films. We report here a convective assembly process for the formation of large-area self-assembled monolayers of silica microspheres on glass, quartz, and silicon substrates. The structure of the self-assembled monolayers and their spatial extent are significantly influenced by sphere concentration in the suspension, dispersed suspension volume, solvent, coating plate speed, and wedge angle. Glass substrates up to $150 \times 150\,mm^2$ are uniformly coated with monolayers of 2-μm silica spheres. It is found that the spherical coating improves the transmittance of quartz wafer from 89.2% to 92.7% around 400 nm and from 90.8% to 92.5% around 1100 nm, demonstrating its broad-spectrum nature. The spherical structure offers an attractive solution to antireflection in crystalline silicon solar cells, as well as thin-film, quantum dot, organic, and flexible solar cells.

1. Introduction

Surface texturing by solution deposition has been recently proposed for omni-directional antireflection in solar cells [1,2]. Theoretical and experimental investigation has been carried out to demonstrate and understand the performance of the microscale surface texture for antireflection. Close to zero reflection can be achieved in the microstructured surface over an extended spectral region for a large range of light incident angle. The surface texture is formed by a monolayer of spherical microparticles of an optically-transparent material partially immersed into a dielectric film with a thickness less than the diameter of the spheres. The unique way in which the surface texture is formed allows it to be prepared from solution, which is inherently low cost and can be applied to different types of solar cells as an add-on coating.

A key issue in preparing the spherical coating is the formation of large area, uniform, and closely packed monolayers of microspheres. Different self-assembly processes can be in principle used to achieve this goal, such as spin coating [3,4], dip coating [5–7], layer-by-layer assembly [8,9], soft lithography [10,11], and evaporation-induced self-assembly [12]. Integration of the spherical coating into large-volume production of commercial solar cells requires the development of a rapid, inexpensive, and well-controlled coating process for the formation of monolayer microspheres. Convective self-assembly was originally developed for controlled deposition of micro- and nanoparticles by Denkov et al. [13,14], and later modified for a more scalable setup by Prevo and Velev [15–17]. Ordering in convectively-assembled colloidal particles has been investigated for various cases ranging from ring formation in drying droplets [18–22], to ordered deposits on the periphery of holes from dewetting films [23], to colloidal crystal formation in thin wetting films [24–29] and ultrathin mesoporous silica films [30]. However, little is known about convective assembly of microscale particles. The relation between coating parameters and structural characteristics of assembled microsphere monolayers is not well understood. In addition, the process has yet to be scaled up into a practical technology. Large-area uniform coatings of microsphere monolayers are important for the performance of the spherical coating.

We report here a convective assembly process for the formation of large-area self-assembled monolayers of silica microspheres on glass, quartz, and silicon (Si) substrates. Various coating parameters have been investigated, including coating plate speed, particle concentration in the suspension, dispersed

* Corresponding authors at: Department of Electrical Engineering, NanoFAB Center, University of Texas at Arlington, Arlington, TX 76019-0072, USA. Tel./fax: +1 817 272 1227.
E-mail addresses: yhwang@uta.edu (Y. Wang), wzhou@uta.edu (W. Zhou), mtao@uta.edu (M. Tao).
[1] Tel.: +1 817 271 8675; fax: +1 817 272 1227.
[2] Tel.: 1+817 272 1353; fax: 1+817 272 7458.

0927-0248/$ - see front matter © 2008 Elsevier B.V. All rights reserved.
doi:10.1016/j.solmat.2008.08.008

suspension volume, solvent, and wedge angle. Parameters which allow the formation of large area, uniform, and closely packed monolayers of silica microspheres have been identified. In addition, spherical coatings for antireflection have been demonstrated by solution deposition on quartz substrates.

2. Experimental

2.1. Materials

The suspension of monodispersed silica mircospheres with a diameter of 2 μm was supplied by Microspheres-Nanospheres, a Corpuscular Company. The suspension was used without further purification. The spin-on glass (SOG), Accuglass® T-11, with a specified thickness range of 0.16–0.26 μm was supplied by Honeywell. Glass slides of 1-mm thick from Fisher Scientific, Si wafers of 500-μm thick from Nova Electronic Materials, and quartz wafers of 500-μm thick from University Wafers were used as substrates. Glass substrates were dipped in a mixture of 30% H_2O_2 and 70% H_2SO_4 at 22 °C and 40% relative humidity for 24 h, rinsed with deionized water, and then preserved in deionized water. The cleaned glass substrates were finally blown dry using N_2 before use. Si and quartz substrates were immersed in acetone for 10 min, rinsed with acetone and isopropyl alcohol, and then dried using N_2.

2.2. Monolayer formation

Our experimental setup for convective assembly is similar to that of Prevo and Velev [14]. A typical convective assembly process is as follows. The silica mircosphere suspension is agitated in an ultrasonic bath and with a magnetic stirrer before use. A controlled amount of suspension is injected into the wedge formed between substrate and coating plate and is entrapped there by capillarity. The coating plate is moved at a programmed speed, thus the liquid meniscus is dragged horizontally across the substrate surface. Microspheres are deposited from meniscus to substrate during the motion. Our coating process is performed at 22 °C and 30–40% relative humidity. The wet coating is air dried in ambient conditions. Various coating parameters have been investigated, such as microsphere concentration in the suspension (5–16 wt%), coating plate speed (0.01–0.25 mm/s), dispersed suspension volume (20–90 μL), wedge angle (20–40°), and solvent (ethanol or water).

2.3. Omni-AR coating

Spherical coatings are formed by spin coating a film of SOG onto substrates with silica microsphere monolayers at 1000 rpm for 30 s, and then heated on a hot plate at 110 °C in air for 1 min to remove solvent and to cross link the SOG film. Some coatings are annealed in a furnace up to 500 °C to investigate the effect of temperature on their performance. Transmittance and reflectance of the spherical coatings are measured under normal incidence using a JASCO V570 UV/vis spectrophotometer in the spectral range of 400–1200 nm. An integrating sphere is used for the measurements of total reflection by collecting all the specular and diffusive components of reflection. The microstructure of the coatings is studied with a Zeiss SUPRA 55VP scanning electron microscope, a Nikon LV100 optical microscope with a digital camera, and laser diffraction.

3. Results and discussion

3.1. Plate speed, dispersed volume, and particle concentration

The effect of coating plate speed on the formation of silica mircosphere monolayers has been investigated, ranging from 0.01 to 0.25 mm/s. It is found that there is a limited range of optimal speed in which large-area uniform monolayers of silica

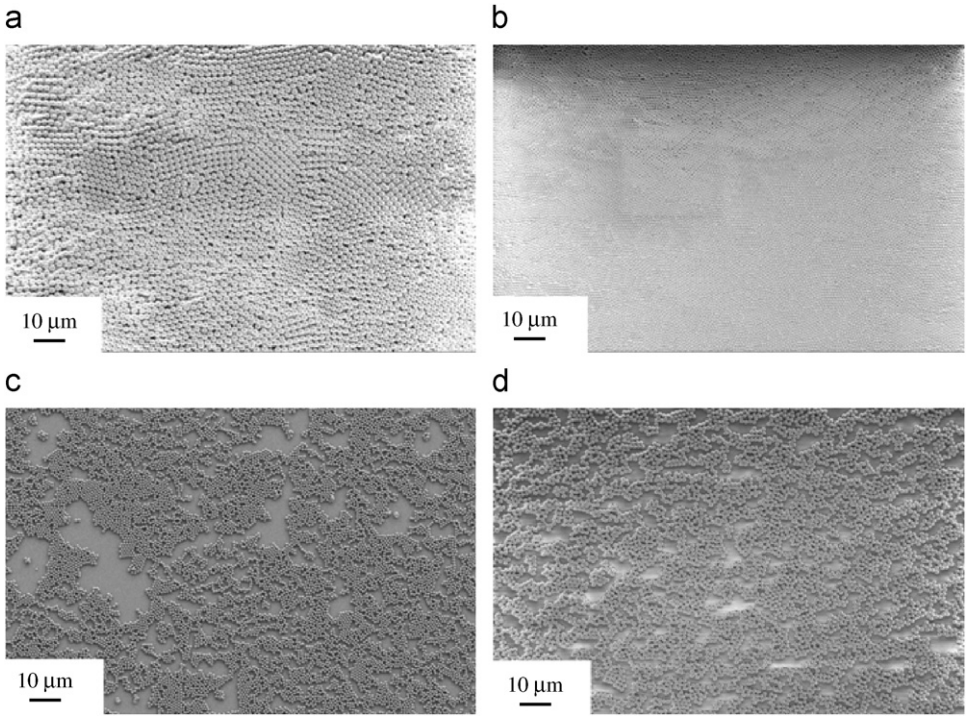

Fig. 1. SEM images of water-dispersed 2-μm silica microspheres at different coating plate speeds. Other coating parameters include 16 wt% particle concentration, 30 μL dispersed volume, and 25° wedge angle on glass substrates. (a) 0.02 mm/s; (b) 0.04 mm/s; (c) 0.07 mm/s; and (d) 0.09 mm/s.

microspheres form. Shown in Fig. 1 is a series of SEM images of coatings of silica microspheres dispersed in water at 16 wt% concentration, 30 μL dispersed volume, and 25° wedge angle on glass substrates. Low plate speed (0.02 mm/s) results in large areas of bilayer and multilayer coatings with poor packing regularity, as shown in Fig. 1a. Further decrease in plate speed leads to multilayers of particles visible to naked eyes. When the plate speed increases to 0.04 mm/s, large areas of uniform closely packed monolayers of silica microspheres are formed (Fig. 1b). With further increase in plate speed, submonolayer coatings are observed consisting of clusters of tens or hundreds of microspheres scattered on the substrate (Fig. 1c and d). The microparticles in the clusters exhibit chaining and short-range ordering. This structure is likely formed when the particles in the drying film are attracted to each other by capillary forces.

During the process of convective assembly, arrays of particles are formed in the meniscus through a convective flux generated by the evaporation of solvent and by the lateral capillary forces. For the formation of a regular and continuous two-dimensional particle monolayer onto a substrate, the plate speed should be equal to the rate of particle array formation [24]. Our experiments indicate that 0.04 mm/s is approximately equal to the rate of array formation in this case. A high plate speed makes it difficult to sustain closely packed monolayers, thus loosely packed submonolayers are formed (Fig. 1c and d). On the other hand, a low plate speed accumulates particles (Fig. 1a) and multilayers of particles are formed.

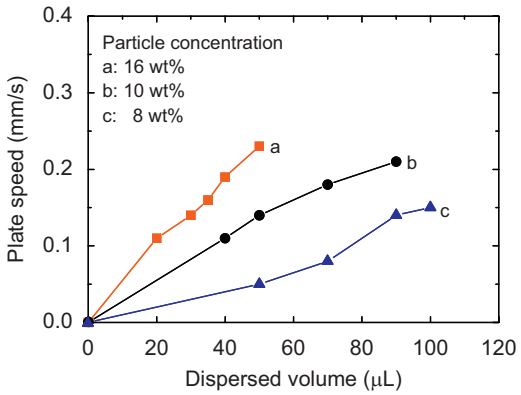

Fig. 2. Dependence of plate speed on particle concentration in ethanol and on dispersed volume for the formation of large area, uniform, and closely packed monolayers on glass substrate. The concentration of silica microspheres: (a) 16 wt%; (b) 10 wt%; and (c) 8 wt%.

Shown in Fig. 2 is the dependence of plate speed on microsphere concentration in ethanol and on dispersed volume for the formation of large area, uniform, and closely packed monolayers of silica microspheres on glass substrate. These are experimentally determined coating parameters. Relatively uniform monolayers of silica microspheres on the entire substrate of $75 \times 25\ mm^2$ in size are obtained under proper conditions. The top-left region (high plate speed and low dispersed volume) in Fig. 2 corresponds to submonolayers as shown in Fig. 1c and d. The lower-right region (low plate speed and high dispersed volume) corresponds to multilayer coatings. It is also found that uniform closely packed monolayers are more likely to be achieved with higher plate speed. It is possible that a higher plate speed minimizes the impact of sedimentation of silica microspheres due to gravity, which is unique to microparticles. Large area, uniform, and closely packed monolayers of silica microspheres are also obtained on quartz and Si substrates.

Fig. 3a (top) is a photograph showing a uniform monolayer of 2-μm silica microspheres on glass substrate of $75 \times 25\ mm^2$ in size. The coating appears translucent due to scattering when viewed in diffuse ambient light, but the color of diffraction from the coating changes when viewed from different angles with directional white light source incident on the coated surfaces. The color change is due to optical diffraction from the ordered monolayer array of silica microspheres. The homogeneous color of the coating demonstrates its uniformity. Laser diffraction can be used to study the structure of two-dimensional self-assembled monolayers [8]. Fig. 3a (bottom) shows diffraction patterns of a laser beam through coatings of silica microspheres. The laser beam is normally incident on the samples with a large beam size of 2 mm and a pinhole diameter of 0.5 mm. The bottom left in Fig. 3a is a set of sharp concentric circles pointing to a well-ordered but multi-domain monolayer, each domain smaller than the beam size. The bottom right in Fig. 3a is a set of regular hexagonal spots corresponding to diffraction from a single closely packed hexagonal domain. Fig. 3b shows an optical microscopy image at 500× magnification of silica microspheres on Si substrate. The monolayer of 2-μm silica microspheres covers a large area with a uniform and closely packed structure, although it appears to be multi-domain.

A series of SEM images taken on the same sample but at different magnifications are shown in Fig. 4. The monolayer is hexagonal in structure and looks sufficiently uniform and closely packed. This can be illustrated by the two-dimensional Fourier

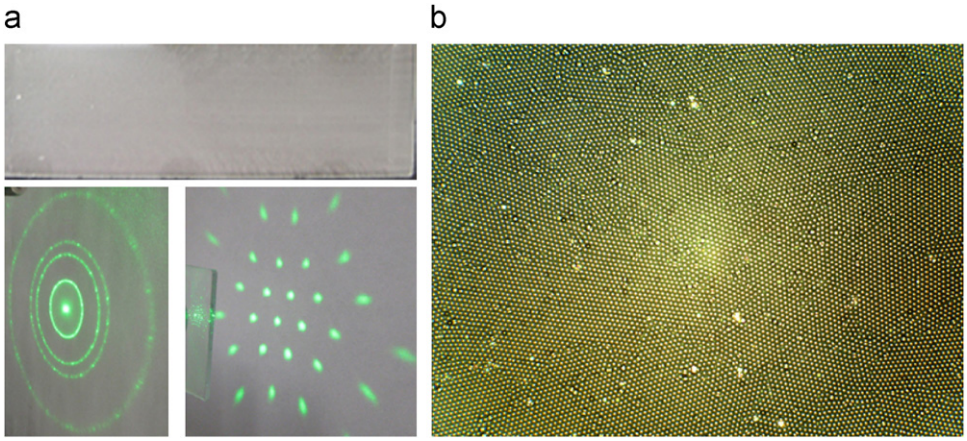

Fig. 3. (a) Photograph of 2-μm silica microsphere monolayer on glass substrate of $75 \times 25\ mm^2$ in size (top) and diffraction patterns of a laser beam through silica microsphere coatings (bottom); (b) optical microscopy image at 500× magnification of silica microsphere monolayer on Si substrate.

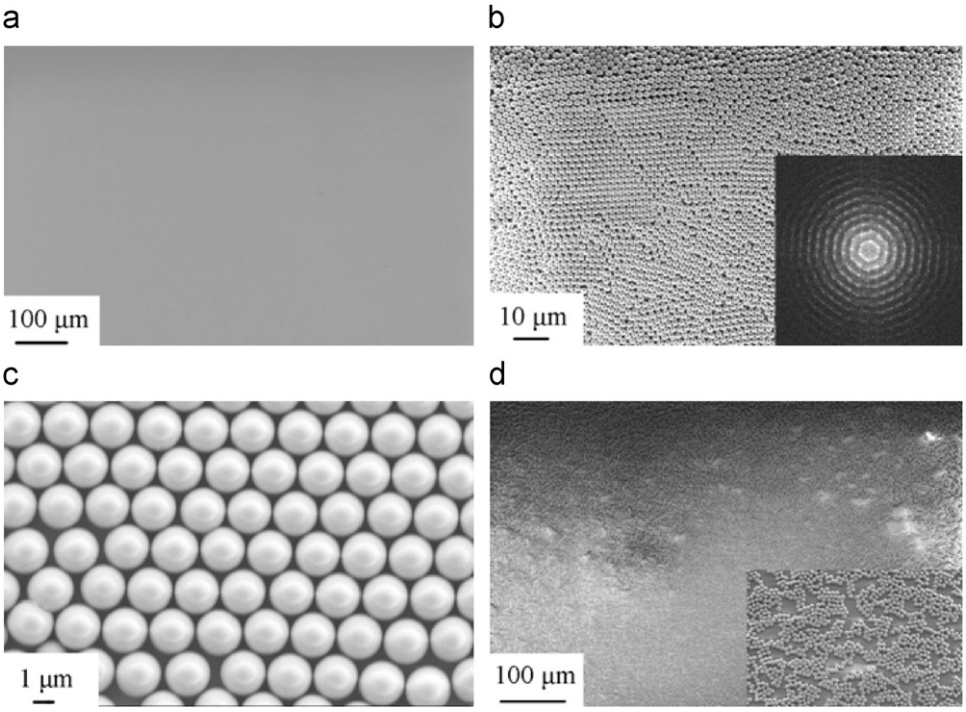

Fig. 4. (a–c) Series of SEM images at different magnifications of silica microspheres on Si substrate and two-dimensional Fourier transform of a low-magnification SEM image (inset in (b)); (d) SEM image along the side of coated Si substrate and high-magnification SEM image of the same location (insert in (d)).

transform of a low-magnification SEM image (inset in Fig. 4b). The sharp peaks confirm the presence of long-range ordering. It should be noted that the hexagonal closely packed structure is not obtained on the entire substrate in this case. Small areas of submonolayers with short-range ordering, as shown in Fig. 4d, are observed along the sides and other locations on the substrate. This is attributed to nonuniform distribution of silica microspheres in the meniscus. However, the optical properties of the silica microsphere coatings are satisfactory for antireflection, as discussed in the following section.

The above results prove that under proper conditions, it is possible to form large area, uniform, and closely packed monolayers of silica microspheres. However, it is not easy to maintain the balance between plate speed, particle concentration, and dispersed volume, because both particle concentration and suspension volume decrease gradually as the coating plate moves along the substrate. This causes the coating to increasingly become loosely packed submonolayers. This problem can be solved by continual supply of the suspension to the meniscus, thus a liquid injection system is needed.

3.2. Solvent

Convective assembly is driven by solvent evaporation. Therefore, solvent is one of the critical factors in forming uniform monolayers of silica microspheres, because the solvent controls surface tension and evaporation rate. We choose deionized water and ethanol to investigate the impact of solvent on monolayer formation. The surface coverage of silica microspheres on the substrate, Φ_{SP}, is defined as $\Phi_{SP} = S_{SP}/S$, where S and S_{SP} represent the total substrate area and the area of the substrate covered by silica microspheres, respectively. Experimentally determined Φ_{SP} for both ethanol-dispersed and water-dispersed suspensions is shown in Fig. 5. These samples are fabricated with 16 wt% particle concentration, 25° wedge angle, and 30 μL ethanol-dispersed suspension or 80 μL water-dispersed suspension on glass substrates.

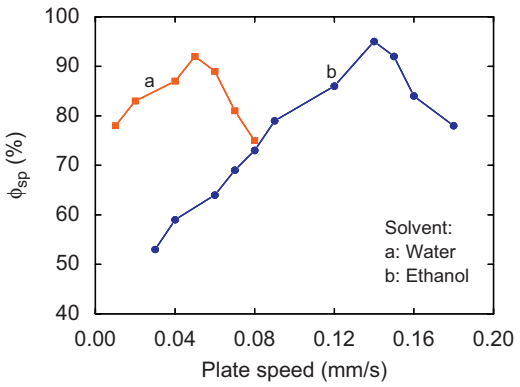

Fig. 5. Impact of plate speed on Φ_{SP} of (a) water-dispersed 2-μm silica spheres and (b) ethanol-dispersed silica microspheres. The samples are prepared with 16 wt% particle concentration, 25° wedge angle, and 30 μL of ethanol-dispersed suspension or 80 μL of water-dispersed suspension on glass substrates.

As seen in Fig. 5, with an increase in plate speed, Φ_{SP} first increases and then decreases for both solvents. In the case of water, uniform monolayers of silica microspheres are obtained with high dispersed volume (80 μL) and low plate speed (0.05 mm/s). In the case of ethanol, uniform monolayers of silica microspheres are obtained with low dispersed volume (30 μL) and high plate speed (0.14 mm/s). It is noted that ethanol-dispersed silica microspheres do not deposit on the substrate when the plate speed is <0.06 mm/s. This suggests that the formation of uniform closely packed monolayers of silica microparticles not only involves lateral capillary forces and convective flux [13,15,21], but also particle-substrate and particle–particle interactions. Our results also indicate that ethanol is a better solvent because it uses less silica microsphere suspension and has higher coating speed.

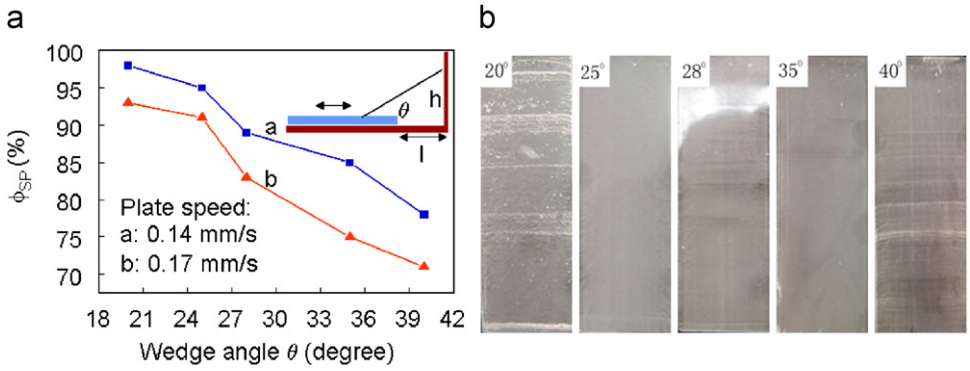

Fig. 6. (a) Impact of wedge angle on Φ_{SP} of ethanol-dispersed 2-μm silica spheres with plate speed of 0.14 mm/s (curve a) and 0.17 mm/s (curve b) and dispersed volume of 30 μL on glass substrate. The insert is a schematic of the coating setup. (b) Photographs of silica microsphere coatings on glass substrates of $75 \times 25\,mm^2$ in size. The samples are prepared with different wedge angles but a constant plate speed of 0.14 mm/s.

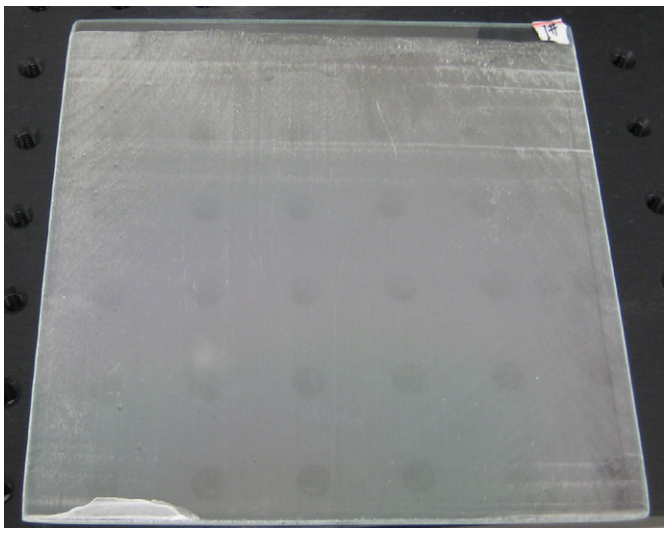

Fig. 7. Photograph of a glass substrate of $150 \times 150\,mm^2$ in size uniformly coated with a monolayer of 2-μm silica microspheres.

3.3. Wedge angle

The wedge angle between substrate and coating plate controls the meniscus angle and dispersed suspension volume. The impact of wedge angle on the formation of silica microsphere monolayers has been investigated. Fig. 6a shows Φ_{SP} of ethanol-dispersed 2-μm silica spheres at different wedge angles. Other coating parameters include plate speed 0.14 mm/s (curve a) or 0.17 mm/s (curve b), dispersed volume 30 μL, and glass substrates. For given plate speed and dispersed volume, Φ_{SP} decreases with increasing wedge angle. For given wedge angle and dispersed volume, Φ_{SP} decreases with increasing plate speed (Fig. 6a). However, lower wedge angles do not help the formation of large-area uniform monolayers of silica microspheres, although higher Φ_{SP} is obtained. Fig. 6b shows photographs of silica microsphere coatings on glass substrates of $75 \times 25\,mm^2$ in size. Multilayers of particles are observed with naked eyes for 20° wedge angle. Relatively uniform monolayers of silica microspheres on the entire substrate are obtained at 25° wedge angle. At 40°, clusters of silica microspheres are observed with a structure similar to Fig. 1c.

With proper conditions, we have obtained large area, uniform, and closely packed monolayers of silica microspheres on glass, quartz, and Si substrates. Fig. 7 is a photograph showing a glass substrate of $150 \times 150\,mm^2$ in size uniformly coated with a monolayer of 2-μm silica spheres. This is the largest substrate we have attempted so far.

3.4. Omni-AR coatings

Shown in Fig. 8 are SEM images of a spherical coating, which comprises a monolayer of 2-μm silica microspheres immersed in a 0.2-μm SOG film on glass substrate. The SOG film is prepared by spin coating. The microspheres arrange themselves into a well-ordered closely packed hexagonal structure (Fig. 8a). The particles are connected by SOG, as compared to particles before SOG (Fig. 4c). No cracks are observed on the entire substrate, indicating little mechanical stress in the coating. The cross-sectional view in Fig. 8b shows a shoulder region at the base of the microspheres due to viscous SOG. These SEM images indicate the successful formation of a spherical coating.

Fig. 9 shows normal-incidence transmittance and reflectance of quartz wafer with a spherical coating. The coatings were annealed at different temperatures up to 400 °C. For comparison, the transmittance of quartz wafer without any coating is also measured. The spherical coating improves the transmittance from 89.2% to 92.7% around 400 nm and from 90.8% to 92.5% around 1100 nm. It also reduces the reflectance from 9.8% to 7.6% around 400 nm and from 7.3% to 6.7% around 1100 nm, demonstrating its broad-spectrum nature. Since the bare quartz wafer already has a high transmittance above 89%, the improvement by the spherical coating is tainted by the high background transmittance. It is worth noting that the absorptance of the spherical coating is $<1\%$ higher than the quartz wafer (data not shown), indicating little or no absorption by the coating in the spectral range of 400–1200 nm. The increase in transmittance at 400 nm (3.5%) is different from the decrease in reflectance (2.2%), which is mostly due to the measurement error associate with the instrument. The most striking feature is the less spectral dependences observed in both transmission and reflection measurements for the sample with coating, which is expected for the spherical structure [2]. It is also worth noting that the reflection measurement is done with the integrating sphere based spectrometer. Thus, the measured reflection is the total reflection, including both specular and diffusive components, for both flat surface (before coating, specular component dominants) and coated textured surfaces (after coating, diffusive component dominants). We also measured transmission and reflection on samples coated only with spherical particles (e.g. Fig. 4, no SOG coating). We observed oscillations on the measured transmission/reflection spectra,

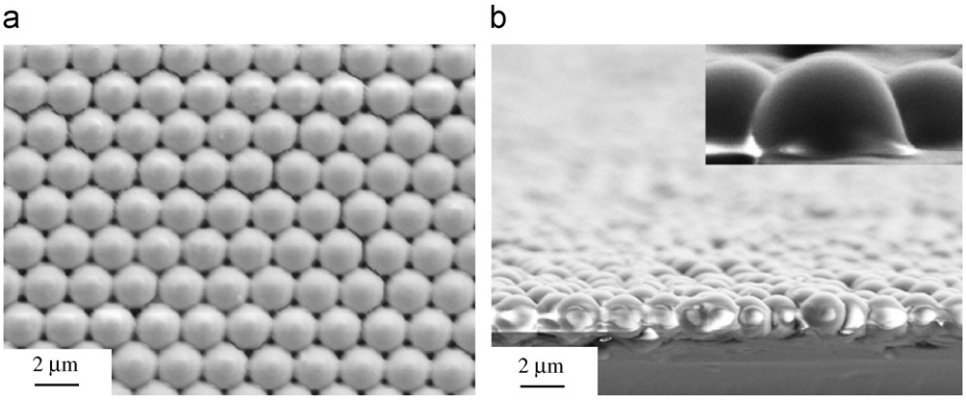

Fig. 8. SEM images of a 2-μm silica sphere monolayer immersed in a 0.2-μm SOG film on glass substrate: (a) top view and (b) cross-sectional view. The insert in (b) is a high-magnification SEM image.

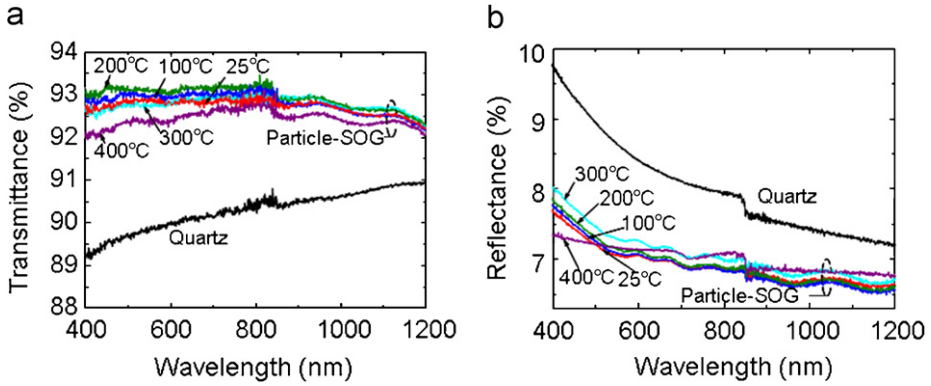

Fig. 9. Measured transmittance (a) and reflectance (b) of quartz substrate coated with a spherical structure, which comprises a monolayer of 2-μm silica spheres immersed in a SOG film of 0.2 μm thick. The coating is annealed at different temperatures up to 400 °C.

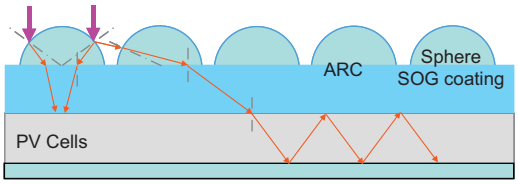

Fig. 10. Reduction of reflection principles in omni-AR coating structure: the ray reflected from the first strike (reflection) hits the spherical surface again (second strike) before reflected away.

which is due to the interference associated with the multiple scattering of close packed spherical particles. Additionally, we observed increased reflection and reduced transmission for the structures with microsphere coating only, as compared to the uncoated quartz sample. This confirms that the effect of omni-AR coating we proposed [1,2]. As shown in Fig. 9, little temperature effect is observed with the coating, suggesting that the coating is purely inorganic, thus stable and transparent, by the process described here.

The mechanism of the reduction in the reflection observed in the structures reported here is similar to the light trapping and second strike effect reported in the single crystal silicon surface textures (pyramid-shaped) [31,32]. Detailed analysis were also given in the earlier publications by the authors [1,2], and is discussed here briefly. As shown in Fig. 10, when incident light strike to the surface of the spherical structure (first strike), portions of reflected beam can strike onto the spherical surface of the neighboring sphere (second strike). This "second strike" or light trapping process results in the reduction of the total reflected power and increased the transmitted power. This principle applied to wavelength-scale surface textures, including pyramid, sphere, and cone-shaped structures [2].

4. Conclusions

We report here a convective assembly process for the formation of large-area self-assembled monolayers of silica microspheres on glass, quartz, and Si substrates. The structure of the self-assembled monolayers and their spatial extent are significantly influenced by particle concentration in the suspension, dispersed suspension volume, solvent, coating plate speed, and wedge angle. Glass substrates up to $150 \times 150\,mm^2$ are uniformly coated with monolayers of 2-μm silica spheres. SEM, optical microscopy, and laser diffraction confirm the formation of large-area uniform monolayers of silica microspheres. Spherical coatings are formed with monolayers of silica microspheres partially immersed into a SOG film with a thickness less than the diameter of the silica spheres. It is found that a spherical coating improves the transmittance of quartz wafer from 89.2% to 92.7% around 400 nm and from 90.8% to 92.5% around 1100 nm, demonstrating its broad-spectrum nature. The spherical coating offers an attractive solution to omni-directional antireflection in current crystalline Si solar cells, as well as future thin-film, quantum dot, and organic solar cells.

Acknowledgments

The authors acknowledge financial support for this work from NSF under Grant no. 0740147, Texas Ignition Fund, and AFRL CONTACT Program. The authors also thank Dr. M. Y. Ali and Mr. K. Han for assistance in annealing experiments and optical characterization.

References

[1] M. Tao, W. Zhou, H. Yang, L. Chen, Surface texturing by solution deposition for omnidirectional antireflection, Appl. Phys. Lett. 91 (2007) 081118-1–081118-3.
[2] W. Zhou, M. Tao, L. Chen, H. Yang, Microstructured surface design for omnidirectional antireflection coatings on solar cells, J. Appl. Phys. 102 (2007) 103105-1–103105-19.
[3] P.K. Biswas, P.S. Devi, P.K. Chakraborty, A. Chatterjee, D. Ganguli, M.P. Kamath, A.S. Joshi, Porous anti-reflective silica coatings with a high spectral coverage by sol–gel spin coating technique, J. Mater. Sci. Lett. 22 (2003) 181–183.
[4] Q.Y. Zhang, J. Wang, G. Wu, J. Shen, S. Buddhudu, Interference coating by hydrophobic aero gel-like SiO_2 thin films, Mater. Chem. Phys. 72 (2001) 56–59.
[5] P. Nostell, A. Roos, B. Karlsson, Optical and mechanical properties of sol–gel antirefective films for solar energy applications, Thin Solid Films 351 (1999) 170–175.
[6] A. Gombert, W. Glaubitt, K. Rose, J. Dreibholz, C. Zanke, B. Blasi, A. Heinzel, W. Horbelt, D. Sporn, W. Doll, V. Wittwer, J. Luther, Glazing with very high solar transmittance, Sol. Energy 62 (1998) 177–188.
[7] D.R. Uhlmann, T. Suratwala, K. Davidson, J.M. Boulton, G. Teowee, Sol–gel derived coatings on glass, J. Non-Cryst. Solids 218 (1997) 113–122.
[8] J. Hiller, J.D. Mendelsohn, M.F. Rubner, Reversibly erasable nanoporous anti-reflection coatings from polyelectrolyte multilayers, Nat. Mater. 1 (2002) 59–63.
[9] J.H. Rouse, G.S. Ferguson, Preparation of thin silica films with controlled thickness and tunable refractive index, J. Am. Chem. Soc. 125 (2003) 15529–15536.
[10] H.Y. Koo, D.K. Yi, S.J. Yoo, D.Y. Kim, A snowman-like array of colloidal dimers for antireflecting surfaces, Adv. Mater. 16 (2004) 274.
[11] H.L. Chen, S.Y. Chuang, Y.H. Lin, Using colloidal lithography to fabricate and optimize sub–wavelength pyramidal and honeycomb structures in solar cells, Opt. Express. 15 (2007) 14793–14803.
[12] A.S. Dimitrov, T. Miwa, K. Nagayama, A comparison between the optical properties of amorphous and crystalline monolayers of silica particles, Langmuir 15 (1999) 5257–5264.
[13] N.D. Denkow, O.D. Velev, P.A. Kralchevsky, I.B. Ivanov, H. Yoshimura, K. Nagayama, Mechanism of formation of two-dimensional crystals from latex particles on substrates, Langmuir 8 (1992) 3183–3190.
[14] B.G. Prevo, O.D. Velev, Controlled, rapid deposition of structured coatings from micro- and nanoparticle suspensions, Langmuir 20 (2004) 2099–2109.
[15] N.D. Denkow, O.D. Velev, P.A. Kralchevsky, I.B. Ivanov, H. Yoshimura, K. Nagayama, Two-dimensional crystallization, Nature 361 (1993) 26.
[16] B.G. Prevo, Y. Hwang, O.D. Velev, Convective assembly of antireflective silica coatings with controlled thickness and refractive index, Chem. Mater. 17 (2005) 3642–3651.
[17] B.G. Prevo, E.W. Hon, O.D. Velev, Assembly and characterization of colloid-based antireflective coatings on multicrystalline silicon solar cells, J. Mater. Chem. 17 (2007) 791–799.
[18] R.D. Deegan, O. Bakajin, T.F. Dupont, G. Huber, S.R. Nagel, T.A. Witten, Capillary flow as the cause of ring stains from dried liquid drops, Nature 389 (1997) 827–829.
[19] R.D. Deegan, O. Bakajin, T.F. Dupont, G. Huber, S.R. Nagel, T.A. Witten, Contact line deposits in an evaporating drop, Phys. Rev. E 62 (2000) 756–765.
[20] R.D. Deegan, Pattern formation in drying drops, Phys. Rev. E 61 (2000) 475–485.
[21] E. Adachi, A.S. Dimitrov, K. Nagayama, Stripe patterns formed on a glass surface during droplet evaporation, Langmuir 11 (1995) 1057–1060.
[22] V.X. Nguyen, K.J. Stebe, Patterning of small particles by a surfactant-enhanced Marangoni-Bénard instability, Phys. Rev. Lett. 88 (2002) 164501-1–164501-4.
[23] P.C. Ohara, W.M. Gelbart, Interplay between hole instability and nanoparticle array formation in ultrathin liquid films, Langmuir 14 (1998) 3418–3424.
[24] A.S. Dimitrov, K. Nagayama, Steady-state unidirectional convective assembling of fine particles into two-dimensional arrays, Chem. Phys. Lett. 243 (1995) 462–468.
[25] A.S. Dimitrov, K. Nagayama, Continuous convective assembling of fine particles into two-dimensional arrays on solid surface, Langmuir 12 (1996) 1303–1311.
[26] P. Jiang, J.F. Bertone, K.S. Hwang, V.L. Colvin, Single-crystal colloidal multilayers of controlled thickness, Chem. Mater. 11 (1999) 2132–2140.
[27] C.D. Dushkin, H. Yoshimura, K. Nagayama, Nucleation and growth of two-dimensional colloidal crystals, Chem. Phys. Lett. 204 (1993) 455–460.
[28] C.D. Dushkin, G.S. Lazarov, S.N. Kotsev, H. Yoshimura, K. Nagayama, Effect of growth conditions on the structure of two-dimensional latex crystals: experiment, Colloid Polym. Sci. 277 (1999) 914–930.
[29] Z.Z. Gu, A. Fujishima, O. Sato, Fabrication of high-quality opal films with controllable thickness, Chem. Mater. 14 (2002) 760–765.
[30] Z. Yuan, D.B. Burckel, P. Atanassov, H. Fan, Convective self-assembly to deposit supported ultra-thin mesoporous silica films, J. Mater. Chem. 16 (2006) 4637–4641.
[31] P. Campbell, M.A. Green, Light trapping properties of pyramidally textured surfaces, J. Appl. Phys. 62 (1987) 243–249.
[32] M.A. Green (Ed.), Third Generation Photovoltaics: Advanced Solar Energy Conversion, Springer, Berlin, 2005.